Reports

The Spectrum of Comet Austin from 910 to 1180 Å

JAMES C. GREEN, WEBSTER CASH, TIMOTHY A. COOK, S. ALAN STERN

A spectrum of comet Austin (1988 c_1) has been obtained from 910 to 1180 Å. Three bright emission lines were detected, including a forbidden oxygen line (1128 Å), which are attributable to radiative pumping of neutral oxygen by solar Lyman β. The relative strengths of the observed features should prove to be a useful diagnostic of the physical conditions and radiation fields in cometary comae. In addition, the absence of strong spectral features from highly volatile species such as He, Ar, or N_2 can be used to place constraints on the thermal environment under which the comet was formed and has been processed.

COMETS HAVE BEEN OBSERVED SPECTROSCOPICALLY for many years, from the infrared through the vacuum ultraviolet, down to approximately 1180 Å. These observations have shown comets to be primarily composed of water and dust, with many other volatiles present as trace constituents. They have revealed that the cometary coma, the gas cloud that surrounds the nucleus, extends for tens of thousands of kilometers into interplanetary space, and can vary in composition and physical conditions across its extent. However, not all elements and molecules can be well studied with observations at wavelengths longer than 1180 Å. Observations at wavelengths shorter than 1180 Å can yield new insights on the physical processes occurring in the comet.

We have developed a far ultraviolet imaging spectrometer, operating from 910 to 1180 Å, for the purpose of observing extrasolar system objects. Because the atmosphere completely absorbs radiation in this wavelength band the instrument must be operated in space. Therefore, it is flown on a sub-orbital sounding rocket, which provides several minutes of observing time above the earth's atmosphere before returning the instrument to earth on a parachute. At present, no satellite exists which can perform spectroscopic observations in this band. This capability will not exist until the launch of the Far Ultraviolet Spectroscopic Explorer (FUSE).

Comet Austin provided a unique opportunity for observation, both because it was bright, and because it is likely that it is a "pristine" comet, that is, it was entering the inner solar system for the first time. Therefore, it should provide good insight for determining the formation processes and subsequent evolution of primordial objects in the outer solar system, where the comet has been residing since its formation.

Comet Austin was observed on 28 April 1990 (GMT = 09:45) with a sounding rocket-borne far-ultraviolet spectrometer launched from White Sands Missile Range. At the time of the observation, comet Austin was at a heliocentric distance of approximately 0.6 AU, and a geocentric distance of approximately 0.6 AU.

The telescope/spectrometer has a resolution of approximately 3 Å and an average effective area of approximately 0.5 cm^2 in the wavelength region from 910 to 1180 Å. The spectrometer entrance aperture is defined by two slits. The primary slit is 9 arc sec by 120 arc sec and the secondary slit is 3 arc sec by 220 arc sec. The spectrum was recorded on an imaging microchannel plate detector. A complete description of the instrument has been published elsewhere (*1*). The instrument was calibrated for absolute effective area and spectral resolution both before and after flight at the far ultraviolet calibration facility at the University of Colorado (*2*).

Comet Austin was observed for 258 s, with the spectrometer entrance slit aligned along the comet's tail. The brightest part of the comet, as seen in the visible, was centered on the primary slit, and the tail of the comet extended along the secondary slit. In Fig. 1 we show all the events recorded on the detector during the observation of comet Austin. Both real photon events and dark background events are displayed. The direction of dispersion and the orientation of the slit on the sky are also depicted. Three bright features are evident in the spectrum of the nucleus, while only one is clearly present in the tail. In Fig. 2 we show the spectrum of the comet from the region within ±1 arc min (approximately ±26,000 km) of the cometary nucleus (the primary slit). The ordinate in Fig. 2 represents total counts collected during the observation, not flux. No correction has been made for background subtraction or instrument response. However, the background signal is very small compared to the bright features, and the instrument response is very flat, so that the ratio of counts in each feature is very close to the flux ratio. The low level counts outside the region of the three bright features is simply integrated detector background, and does not indicate the presence of any continuum emission.

The brightest feature seen in Fig. 2 is HI Lyman β 1025.7 Å, blended with an OI triplet at 1025.7, 1027.4, and 1028.7 Å [$3d\ ^3D_{1,2,0} \rightarrow 2s^2\ 2p^4\ ^3P_{2,1,0}$ (ground state)], radiatively pumped by solar Lyman β. Given the uncertainty concerning the physical conditions within the coma, it is impossible to state at this time what fraction of the emission originates from HI or OI, or both. Additionally, some fraction of the emission originates from geocoronal and interplanetary Lyman β [on the order of 10 rayleighs (R); 1 R = $10^6/4\pi$ photons $cm^{-2}\ s^{-1}\ sr^{-1}$)]. The intensity of the blended OI and HI feature is approximately 1100 R. Fluorescent pumping of OI by solar Lyman β was originally predicted by Bowen (*3*), and has been identified through bright OI 1304 Å emission in two previous comets, Khoutek (1973 XII) and West (1976 VI) (*4*). However, to our knowledge, this is the first time the cometary Lyman β line has been directly observed.

The other two features, which occur at 1042 ± 2 Å and 1127 ± 2 Å have been identified as an OI triplet dominated by 1041.7 Å ($4s\ ^3S_1 \rightarrow 2s^2\ 2p^4\ ^3P_2$) and an OI

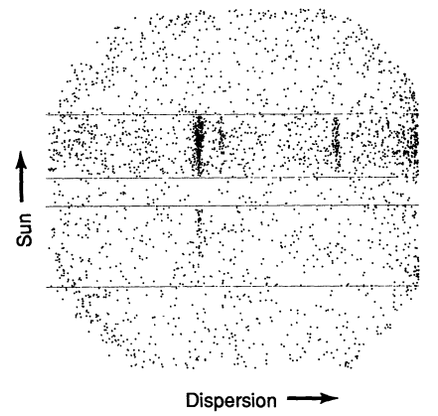

Fig. 1. A plot of all the events recorded during the observation of comet Austin. The numbers 1 and 2 indicate the locations of the primary and secondary slits, respectively. Wavelength increases toward the right. The brightest feature in the primary slit is the feature at 1026 Å. The higher level of background at the extreme right of the detector is due to scattered Lyman α.

Center for Astrophysics and Space Astronomy, University of Colorado, Boulder, CO 80309–0391.

complex near 1128.3 Å ($3p\ ^3P_{1,2,0} \rightarrow 2s^2\ 2p^4\ ^3P_{2,1,0}$). The intensity of the 1042 Å and 1127 Å features are approximately 190 and 320 R, respectively. Other low level emission features may be present near 989 Å (OI) and 1134 Å (NI), however, the statistical significance of these features is low, and further analysis is required.

It is also interesting to note the absence of any significant emission features associated with highly volatile noble gases. Argon and helium features would have been expected from transitions at ArI λ 1048, 1066 Å, and HeI λ 584 Å (appearing at 1168 Å in second order). Since comet Austin's orbit indicates that it was making its first approach to the inner solar system at the time of our observation, the absence of any significant emission from these elements may place important limits upon the thermal conditions during the comet's formation and later storage in the Oort cloud (*5*).

In Fig. 3, we show an energy level diagram of OI, indicating the likely transition paths that are indicated by the emission (*6*). The 1042 Å and 1128 Å feature result from the cascade of radiatively pumped OI by solar Lyman β. While the presence of the permitted OI lines near 1042 Å were not unexpected, the existence of the forbidden line at 1128 Å is a surprise. However, we are confident in the identification of this line because (i) there are no permitted ground state transitions of any reasonably abundant elements within the error of the line identification (7), (ii) most molecular processes would be expected to make several lines of comparable strength, rather than the single line observed, and (iii) it would require an extremely unfortunate coincidence to have a non-oxygen feature occur exactly where an OI cascade feature could appear, and no where else, especially when all other observed features are consistent with the OI pumping scenario.

Additionally, we have ruled out the possibility of an instrumental origin for the 1128 Å feature. The feature has the proper signature for line emission from a diffuse source, and therefore the only reasonable instrumental source for this feature would be a grating ghost from the very bright Lyman α feature at 1216 Å which is outside of this instrument's bandpass. Grating ghosts occur when wavelengths appear at a diffracted angle that is inconsistent with the grating equation. These normally result from fabrication errors in the grating.

There is an independent estimate of the Lyman α intensity from Austin of 150 kR, obtained by scaling IUE measurements. This would mean that there would have to be a ghost of approximately 0.2% to account for the 1128 Å feature. We have ruled out any grating ghosting to a level of 0.03% by laboratory measurements.

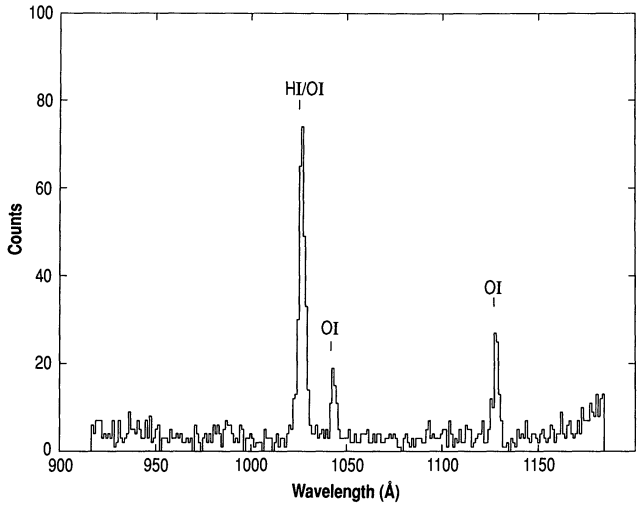

Fig. 2. The spectrum of comet Austin from 910 to 1180 Å. The three bright features noted are the combined hydrogen and oxygen emission near 1026 Å, the permitted oxygen line near 1042 Å, and the forbidden oxygen line near 1128 Å. The *y*-axis represents total counts per bin, which have not been corrected for instrumental response. The slight rise in counts at the extreme right of the plot is due to low level scattered Lyman α.

Another argument against any possible ghosting can be seen in Fig. 1. Because Lyman β is present in both the nucleus and the tail, it is reasonable to assume that Lyman α is present as well. Therefore, any ghost of Lyman α would be expected to appear in the tail with the same intensity relative to Lyman β as seen in the nucleus. But there is no 1128 Å emission seen in the tail, and this non-detection is significant to 98%. This result further indicates that the 1128 Å feature seen in the primary slit is not a ghost.

It is also of interest to note that the presence of forbidden OI emission in comets is not unprecedented. Festou and Feldman (*8*) identified the $^1S \rightarrow {}^3P$ forbidden line of OI at 2972 Å in comet Bradfield. Other forbidden lines of OI have been seen in several other comets (*9*). However, these previously observed lines originated from metastable states, while the 1128 Å feature originates from a state with a permitted path to the ground state. Therefore, the physical implications of this emission are different than those of the previously observed forbidden lines.

The presence of the strong OI 1042 Å emission combined with the lack of accompanying OI 989 Å emission indicates that the fluorescence mechanism previously described is occurring in the coma. However, in order to produce the 1128 Å emission, the coma would have to be very optically thick to λ 8446 Å emission. The number of optical depths in this line would have to be comparable to the 8446/1128 branching ratio, probably of order 10^4. Under such circumstances, 1128 Å emission from the $3p\ ^3P$ state would be expected. In fact, in the extremely optically thick limit, the intensity of any feature should be proportional to the number of possible transitions paths. The 1128 Å feature has eight possible transitions to the ground state, while the 1042 Å feature has only three. Therefore, the 1128 Å feature would be approximately 8/3 as bright as the 1041 Å feature. This ratio is roughly seen in the observation. This ratio should also hold true for any OI λ 1304 Å emission from the comet. This feature is outside of our instrument bandpass, but was observed by another sounding rocket instrument. Preliminary results from that observation indicate that the 1304 Å emission strength was about 100 R over a comparable spatial region. Again, the 1128/1304 ratio is roughly consistent with the extremely optically thick scenario.

Unfortunately, this scenario requires OI densities in the coma that are many orders of magnitude higher than those predicted from standard cometary models. However, we feel that the detection of all three OI lines that could result from a Lyman β pumped cascade indicates strongly that this cascade process is occurring, and that the 1127 ± 2 Å feature is the OI 1128 Å transition. At

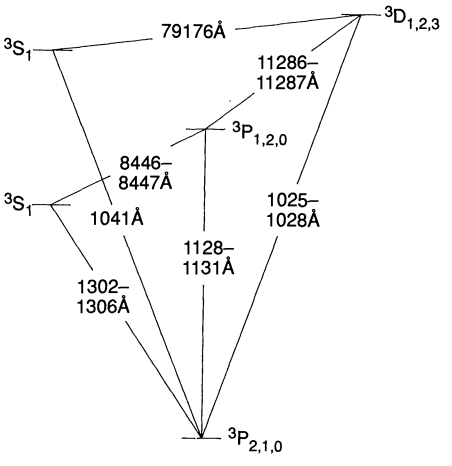

Fig. 3. A partial energy level diagram for OI, showing the relevant transitions that appear in this observation.

present, we cannot give a completely adequate explanation for its presence. There is no other evidence of extremely high densities in the coma. But there are other possible explanations for the emission. For example, following the suggestion of Gladstone (*10*), it is possible that intense electric fields in the coma could change the 1128/8446 branching ratio so that the 1128 Å transition is no longer forbidden. Other possible explanations may exist. However, we want to emphasize that the detection is real, and not due to instrumental effects.

Other astrophysical objects seem to indicate that similar processes are occurring. Thus we may find in the future that the 1128 Å line will become a standard diagnostic for many classes of objects. For example, quasar emission-line clouds have been shown to be optically thick in 8446 Å, an optical line that populates the $3p\ ^3P$ state of OI, the originating state for 1128 Å emission (*11*). M-giant chromospheres have exhibited 1641 Å emission, another forbidden transition resulting from a cascade through the $3p\ ^3P$ state (*12*). Unfortunately, observations of these dim targets at 1128 Å will probably have to wait until the FUSE experiment flies.

REFERENCES AND NOTES

1. W. Cash *et al.*, *Exper. Astron.* **1**, 123 (1989).
2. T. A. Cook, W. Cash, J. C. Green, in preparation.
3. I. S. Bowen, *Pub. A.S.P.* **59**, 196 (1947).
4. P. D. Feldman *et al.*, *NASA Special Publication SP-393* (NASA, Washington, DC, 1974), p. 773.
5. S. A. Stern, thesis, University of Colorado (1989).
6. S. Bashkin and J. Stoner, *Atomic Energy Levels and Grotrian Diagrams* (North-Holland, Amsterdam, 1975), vol. 1.
7. There is an allowed transition from the $7d\ ^3P$ state of CI within the allowed error in the wavelength identification, however, it is unlikely that this could be the source of the emission, given the lack of accompanying lines out of the $8d\ ^3P$ or $6d\ ^3P$ states.
8. M. C. Festou and P. D. Feldman, *Astron. Astrophys.* **103**, 154 (1981).
9. P. Swings, *Annal. Astrophys.* **25, 165 (1962).**
10. R. Gladstone, private communication.
11. S. Grandi, *Astrophys. J.* **268**, 591 (1983).
12. A. Brown, M. Ferraz, C. Jordan, *The Universe at Ultraviolet Wavelengths: The First Two Years of IUE*, R. D. Chapman, Ed. (NASA CP-2171), (NASA, Washington, DC, 1981), p. 297.

13. The authors thank J. Van Overeem of the NASA/Wallops Island Flight Facility for his invaluable assistance in making this observation possible. We would also like to thank P. Feldman, M. Shull, T. Snow, and J. Stocke for useful scientific discussions and D. Yeomans for providing accurate and up-to-date orbital elements for comet Austin. This work was supported under NASA grant NSG 5303.

25 May 1990; accepted 20 November 1990

Phase Transition and Thermal Expansion of $MgSiO_3$ Perovskite

YANBIN WANG, DONALD J. WEIDNER, ROBERT C. LIEBERMANN, XING LIU, JAIDONG KO, MICHAEL T. VAUGHAN, YUSHENG ZHAO, AMIR YEGANEH-HAERI, ROSEMARY E. G. PACALO

Results from in situ x-ray diffraction experiments with a DIA-type cubic anvil apparatus (SAM 85) reveal that $MgSiO_3$ perovskite transforms from the orthorhombic *Pbnm* symmetry to another perovskite-type structure above 600 kelvin (K) at pressures of 7.3 gigapascals; the apparent volume increase across the transition is 0.7%. Unit-cell volume increased linearly with temperature, both below (1.44×10^{-5} K^{-1}) and above (1.55×10^{-5} K^{-1}) the transition. These results indicate that the physical properties measured on the *Pbnm* phase should be used with great caution because they may not be applicable to the earth's lower mantle. A density analysis based on the new data yields an iron content of 10.4 weight percent for a pyrolite composition under conditions corresponding to the lower mantle. All current equation-of-state data are compatible with constant chemical composition in the upper and lower mantle; thus, these data imply that a chemically layered mantle is unnecessary, and whole-mantle convection is possible.

AT PRESSURES GREATER THAN 23 GPa, all of the major minerals of the earth's upper mantle transform under high temperatures to phase assemblages dominated by $(Mg,Fe)SiO_3$ perovskite (*1*). Therefore, the properties of this silicate perovskite control those of the earth's lower mantle (depths of 650 to 2900 km) and knowledge of its crystal structure and response to changes in temperature and pressure are crucial in understanding physical and chemical processes of the mantle. Under ambient conditions, the crystal structure of the metastable perovskite is orthorhombic, with space group *Pbnm* (*2*), which has been assumed to be the stable structure throughout the lower mantle. However, many perovskite-structure materials with ABO_3 composition undergo sequences of phase transitions with increasing pressure and temperature, and these transitions are associated with dramatic changes in physical properties (*3*). Earlier conclusions that the *Pbnm* distortion remains unchanged with increasing temperature and pressure (*4, 5*) have been shown to be incorrect (*6–9*). Transmission electron microscopy studies on twin-domain structures in $MgSiO_3$ perovskite quenched from 26 GPa and 1873 K provide indirect evidence of the presence of structural phase transitions (*10*). At atmospheric pressure thermal expansion measurements have been limited to a few hundred kelvin, above which the perovskite structure becomes unstable (*4, 6, 9*). Recently, Mao *et al.* (*11*) carried out a simultaneous high-pressure and high-temperature study using an externally heated diamond-anvil cell; however, as the temperature was increased from 300 to 877 K, the pressure decreased from 27 to 4 GPa.

By using a large-volume, high-pressure apparatus in conjunction with a synchrotron x-ray source, we have been able to stabilize $MgSiO_3$ perovskite to temperatures up to 1253 K at constant pressure and to study the evolution of its crystal structure by x-ray diffraction. The experiment was performed in a DIA-6–type cubic-anvil apparatus (SAM-85) at the superconducting wiggler

Mineral Physics Institute and Department of Earth and Space Sciences, State University of New York at Stony Brook, Stony Brook, NY 11794.

Table 1. Zero-pressure linear compressibilities of $(Mg,Fe)SiO_3$ perovskite at 300 K. P_{max}, maximum pressure in the measurements; pressure medium: M-E, methanol-ethanol; M-E-W, methanol-ethanol-water; Ne, neon; sample form: SC, single crystal; P, powder. References (*7*), (*8*), and (*11*) give angle-dispersive x-ray data from the diamond cell; (*16*) gives Brillouin spectroscopy data at 1 bar.

β_a (TPa^{-1})	β_b (TPa^{-1})	β_c (TPa^{-1})	P_{max} (GPa)	x	Pressure medium	Sample	References
1.31	1.20	1.56	0	0	—	SC	(*16*)
1.41	1.07	1.57	10	0	M-E-W	SC	(*8*)
1.30	1.04	1.24	13	0	M-E, Ne	SC	(*7*)
1.29	1.05	1.33	30	0 to 0.2	Ne	P	(*11*)
1.29	1.03	1.31	7.3	0	NaCl	P	This study